

ChemComm

Chemical Communications

Accepted Manuscript

This article can be cited before page numbers have been issued, to do this please use: M. Huang, J. Dong, Z. Wang, Y. Li, L. Yu, Y. Liu, G. Qian and S. Chang, *Chem. Commun.*, 2020, DOI: 10.1039/D0CC05602B.



This is an Accepted Manuscript, which has been through the Royal Society of Chemistry peer review process and has been accepted for publication.

Accepted Manuscripts are published online shortly after acceptance, before technical editing, formatting and proof reading. Using this free service, authors can make their results available to the community, in citable form, before we publish the edited article. We will replace this Accepted Manuscript with the edited and formatted Advance Article as soon as it is available.

You can find more information about Accepted Manuscripts in the [Information for Authors](#).

Please note that technical editing may introduce minor changes to the text and/or graphics, which may alter content. The journal's standard [Terms & Conditions](#) and the [Ethical guidelines](#) still apply. In no event shall the Royal Society of Chemistry be held responsible for any errors or omissions in this Accepted Manuscript or any consequences arising from the use of any information it contains.

COMMUNICATION

Revealing the Electronic Structure of Organic Emitting Semiconductors at Single-Molecule level

Received 00th January 20xx,
Accepted 00th January 20xx

Mingzhu Huang, Jianqiao Dong, Zhiye Wang, Yunchuan Li*, Lei Yu, Yichong Liu, Gongming Qian and Shuai Chang*

DOI: 10.1039/x0xx00000x

Revealing the electronic structure of organic emitting molecules is instructive for tuning electron-hole balance, one of the key factors in regulating the organic light emitting diodes (OLED) performance. Herein, we introduced single molecule conductance measurement (SMCM) technology to probe the conductance of three model emitting molecules on Au surface, finding their hole transporting ability across the metal-molecule interface can be suppressed after electron-withdrawing arms are connected to the center component. This observation would benefit the electron-hole balance of the film in large scale (OLED devices) whose holes are excessive relative to electrons. I-V modeling reveals that the conductance drop between molecules is owing to reduced metal-molecule coupling rather than the impaired energy level alignment. The electronic structure variation between molecules could also be revealed by photophysical measurement, electrochemical analysis, and density functional theory (DFT) simulation, which give supportive evidence to the SMCM result.

Traditional organic emitting devices are generally composed of several layers which would inevitably face complicated fabrication processes. To circumvent this problem, devices of simple structures depositing active materials directly onto electrodes of inorganic ingredient without the injection or transporting layers are proposed to reduce the difficulty of realizing industrial applications^[1]. As a consequence, investigating and understanding the charge transport behavior of organic emitting molecules on the metal surface will be important for the designed materials. Up to date, researchers in such fields mainly rely on DFT simulations to examine the electronic performance of different structured molecules in guiding the molecular design of organic emitting semiconductors^[2]. Although single-molecule electrical properties (e.g., molecular conformations or orbital distributions) can be predicted in the modeling, the simulation is generally performed in vacuum, which may deviate significantly from the real ambient condition at the film surface.

Therefore, a comprehensive experimental study of the charge transfer processes in organic emitting molecules on metal surface could be critical, which however, has not been reported to date.

SMCM based on scanning tunnelling microscopy break junction (STM-BJ) technique is an effective method widely adopted to investigate the charge transport properties of single molecules between metal electrodes (also called metal-molecule-metal junctions) via statistical analysis of the repeated current-displacement measurements^[3, 4]. Various types of small organic molecules have been successfully incorporated into metal-molecule-metal circuits to research their molecular conductance and electrical behavior on the metal surface^[3, 5]. However, most of these organic molecules investigated to date are non-functional, with their structures mainly constituting of alkyl chains^[4b, 6], benzene oligomers^[7] or thiophene oligomers^[8], whose electronic structure has a large band gap between the highest occupied molecule orbitals (HOMO) and the lowest unoccupied molecule orbitals (LUMO). By contrast, organic emitting molecules are usually made up of rigid conjugated structures^[9], whose electronic conductance properties has not been reported due to lacking chemical anchors required to stably coordinate with the metal electrodes and form well-defined metal-molecule-metal junctions. Chemical modification to introduce the required linkers to the original structures can be a solution, but the extra anchors are usually unnecessary compositions, which could even impair the device performance. To solve this problem, the structural feature of organic emitting semiconducting materials should be analysed.

Typically, the molecular structures of emitting molecules are constructed from the electron-rich donor (D) and electron-deficient acceptor (A) to produce highly emitting-efficient D-A structures^[10]. Typical D moieties, such as triphenylamine (TPA)^[11], carbazole (Cz)^[12] and acridine^[13], have no metal-binding groups and could not be stably functionalized on the metal surface. In contrast, some A moieties (e.g., cyano (-CN)^[14] and pyridine^[15]) can form stable contacts with Au electrodes. Motivated by these evidences, we propose to synthesize a series of A-D-A type functional molecules, adopting TPA as the core and phenyl nitrile groups as the arms. As shown in **Scheme S1 (ESI)**, one to three phenyl nitrile groups were connected to TPA center by substituting the H atoms at the para-position of TPA via Suzuki reactions. Three target structures, 4'-(diphenylamino)-[1,1'-biphenyl]-4-carbonitrile, 4',4''-

The State Key Laboratory of Refractories and Metallurgy, and Institute of Advanced Materials and Nanotechnology, Wuhan University of Science and Technology, Wuhan 430081, China; Email: yc.l@wust.edu.cn; schang23@wust.edu.cn

Electronic Supplementary Information (ESI) available: [NMR, MalDI-ToF, 2D conductance-distance, 1-D conductance histogram, Energy levels]. See DOI: 10.1039/x0xx00000x

(phenylazanediy)bis((1,1'-biphenyl)-4-carbonitrile) and 4',4''',4''''-nitrilotris((1,1'-biphenyl)-4-carbonitrile)), respectively denoted as CN-TPA, DCN-TPA, and TCN-TPA are successfully synthesized via the route shown in **Scheme S1** (see Supporting information S1).

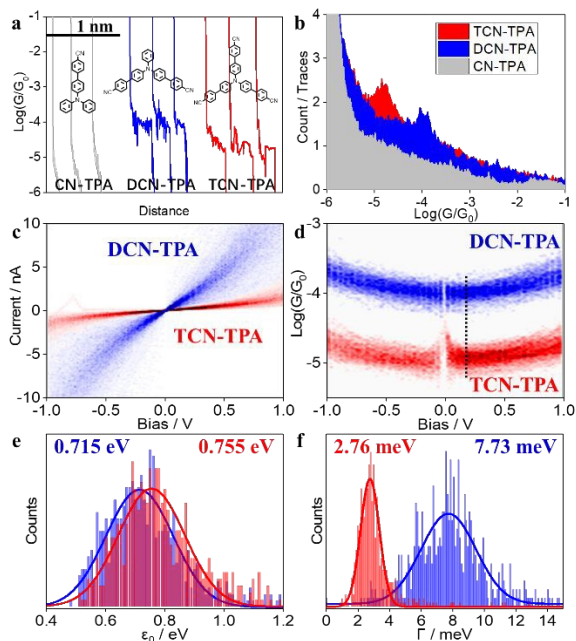


Figure 1 Sample conductance traces (a) and conductance histograms (b) for CN-TPA (grey), DCN-TPA (blue), and TCN-TPA (red). (c, d) 2D I-V / G-V distribution for DCN-TPA (blue) and TCN-TPA (red). (e, f) The statistics of energy level difference and values of electronic couplings.

Single-molecule electronic conductance of three target molecules is investigated using STM-BJ technique, which was much described previously^[16]. Distinctive plateau features are often observed in the current decay traces when the objective molecule bridges both Au electrodes^[3a, 7a, 17]. As shown in Figure 1a, several typical current decay traces recorded with substrates modified with DCN-TPA (blue traces) and TCN-TPA (red traces) show clear plateaus in the conductance range around $10^{-3} \sim 10^{-5} G_0$ ($G_0 = 2e^2/h$). In contrast, no distinctive features are observed in the sharp-decay curves for CN-TPA modified substrates (grey traces), indicating no stable metal-molecule-metal junctions can be formed for CN-TPA with a single binding group. Histograms of combined traces in Figure 1b show only a smooth background for CN-TPA occupied junctions. However, well defined conductance peaks can be generated for DCN-TPA and TCN-TPA modified junctions, with their most probable single-molecule conductance centered at $10^{-3.9} G_0$ (9.76 nS) and $10^{-4.7} G_0$ (1.55 nS) respectively. Repeated measurements are carried out with platinum electrodes, giving essentially identical results for three molecules (see details in ESI Figure S1). Two-dimensional conductance versus relative distance histograms show similar junction elongation length for both DCN-TPA and TCN-TPA (see circled region in Figure S2), suggesting similar structural configurations are being formed inside the gap, each with two -CN groups bridging both electrodes.

Despite the very close conduction path, the measured electronic conductances for two molecules are quite different. Comparing with DCN-TPA, the additional phenyl nitrile substituent

on TCN-TPA brings down its conductance by almost an order of magnitude. The electron-withdrawing property of this A-type substituent is known to be able to lower the HOMO with respect the gold Fermi energy (E_F)^[18]. The decreased conductance in TCN-TPA might suggest a HOMO-facilitated transport, in which the electron-withdrawing moiety extends the energy difference between E_F and the conduction orbital. To better understand the charge transport mechanism of these A-D-A type functional molecules, we performed the current-voltage (I-V) characteristics of single-molecule junctions, which provides significantly more information beyond a fixed low-bias conductance measurement (Figure S3, ESI)^[19]. Figure 1c shows the two dimensional (2D) I-V distributions for both types of molecular junctions, each constructed from combined measurements of more than 500 I-V curves. For both cases, the current increases linearly with bias over a small bias range (around ± 0.3 V). At higher bias voltages, nonlinear I-V response is evident. By converting current I into conductance G via $G=I/V$, a 2D G-V plot can be generated as Figure 1d, showing clearly the voltage dependence of the measured molecular junction conductance. Two bowl-shaped bands show conductance discrepancy of up to an order of magnitude between two molecular systems, consistent with the break-junction result. In addition, both molecules exhibit constant conductance below ~ 0.3 V, and their conductance rising with increasing bias above this threshold. Statistical analysis of the vertical distribution of G values at 0.1V (dashed line) reveals molecular conductance of $10^{-3.9} G_0$ and $10^{-4.6} G_0$ for DCN-TPA and TCN-TPA (Figure S4), very close to that obtained in the break junction measurement, showing that each I-V curve preserves the conductance information of single molecules at a given bias.

By fitting each I-V curve with a single level tunneling model^[20]:

$$I(V) = \frac{2e\Gamma}{h} \left\{ \tan^{-1} \left[\frac{eV/2 - \epsilon_0}{\Gamma} \right] + \tan^{-1} \left[\frac{eV/2 + \epsilon_0}{\Gamma} \right] \right\}, \quad (1)$$

two essential parameters Γ and ϵ_0 , which implicates the metal-molecule contact configurations in molecular junctions, can be obtained statistically. ϵ_0 denotes the energetic alignment of the molecular frontier orbital with respect to the E_F and Γ represents the metal-molecule electronic coupling energy^[21]. Figure 1e shows the overlaid distribution of ϵ_0 for two molecular systems. The three-armed TCN-TPA show slightly larger ϵ_0 than two-armed DCN-TPA, which could be attributed to the additional arm that withdraws electrons from the TPA center and lowers its occupied molecular orbitals. This enlarged energy difference ϵ_0 from DCN-TPA to TCN-TPA once again suggests that charge is transported through HOMO as the conducting orbital. The metal-molecule couplings Γ for both types of molecular junctions are quite small compared to that of reported thiol linkers (up to 130 meV)^[22], reflecting the weakly binding nature of -CN groups toward the metal electrodes, consistent with a previous report^[23]. However, the electronic coupling energy measured in DCN-TPA junctions is much different (~ 3 times) from that obtained in TCN-TPA junctions, despite the identical -CN metal binding groups (Figure 1f). As suggested^[22], the electronic coupling strength is not only anchoring-dependent but also relying on other factors such as the electronic details of the molecular backbone. In our case, we speculate that the extra electron-withdrawing phenyl nitrile arm in TCN-TPA reduces the electron occupation of the TPA core, thereby impacting the electronic hybridization between the

core and the other two arms linking the molecule to electrodes. As a result, the electronic interaction between the binding group and the molecular backbone is affected and the resulting metal-molecule coupling strength is thus decreased. From these I-V measurements, we can conclude an A-type substituent on a D-type backbone might impair both ϵ_0 and Γ of the molecular junction. Based on a single-Lorentzian model: $G=G_0/[(\epsilon_0/\Gamma)^2 + 1]$ ^[21], the interplay between ϵ_0 and Γ could greatly impact the measured molecular conductance. Given that ϵ_0 for both molecules are very close, the large variance in Γ between two molecular systems is more decisive in determining their conductance variation.

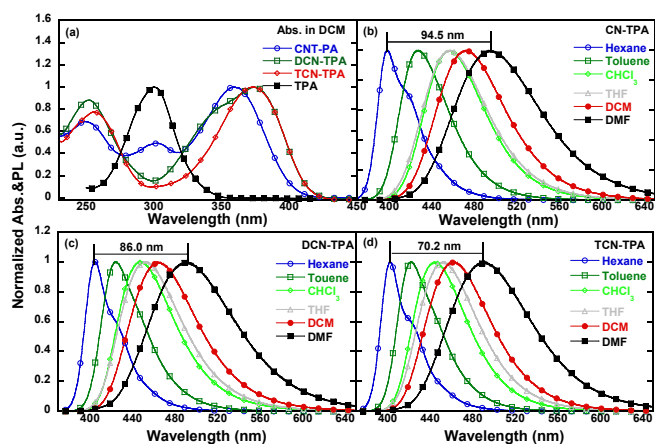


Figure 2 The absorption spectra of TPA (○), CN-TPA (●), DCN-TPA (◆), and TCN-TPA (▼) in DCM (a); and photoluminescence spectra of CN-TPA (b), DCN-TPA (c), and TCN-TPA (d) in various polarized solvents: n-hexane (○), toluene (□), CHCl_3 (◇), THF (△), DCM (●), and DMF (■).

We further performed photo-physical characterization of the synthesized compounds to investigate their electronic structure properties. Figure 2a shows the UV-vis absorption spectra of CN-TPA, DCN-TPA, and TCN-TPA (1×10^{-5} M) measured in dichloromethane (DCM). All three molecules show two similar absorption peaks at 250 and 350-400 nm, which originate from the absorption of their molecular skeleton and the intramolecular charge transfer (ICT) state respectively. Notably, CN-TPA shows an additional absorption peak at 300 nm, which is unseen for DCN-TPA or TCN-TPA. To assign this peak, the absorption spectrum of the TPA core was also measured, showing a peak at the same position as CN-TPA. This implies that the electronic structure of TPA can be affected by the addition of a phenyl nitrile arm in CN-TPA, which could be further changed when more phenyl nitrile arms are added, as suggested by the vanished TPA absorption peak in the spectra for DCN-TPA and TCN-TPA. It indicates that the electron-withdrawing substituents on TPA do induce significant electron redistribution toward the binding groups.

To elucidate the specific role of each individual phenyl nitrile arm, we compared the ICT properties of three molecules by measuring their photoluminescent (PL) spectra in various solvents with different polarity (Figure 2b-d). Obvious solvatochromism is shown for three molecules and their emission spectra exhibit huge bathochromic shifts from nonpolar n-hexane to polar DMF. CN-TPA shows the strongest ICT state accompanied with the largest Stokes shift^[24], implying that the electron-donating ability of TPA core in CN-

TPA is the strongest. With more arms added, the electron-donating behavior of TPA is weakened, as shown in the sequentially reduced Stokes shift for compounds with one, two and three arms. Because the conjugation is disturbed by the central N atom in TPA, their excited states are determined by a basic emitting part from the N atom of TPA to the end of CN^[25], which indicates the same ICT path for three molecules. Therefore, the decreasing ICT intensity from CN-TPA to DCN-TPA and to TCN-TPA can be deemed as a signature of decreasing charge delocalization toward the -CN anchors. The calculated surface charge on the N atom of -CN moiety is -0.315, -0.313, and -0.311 for CN-TPA, DCN-TPA and TCN-TPA, respectively, in agreement with the gradually weakened electron-donating ability of -CN toward the metal electrode, likely explaining their difference in the electronic couplings (Γ) as we discussed previously.

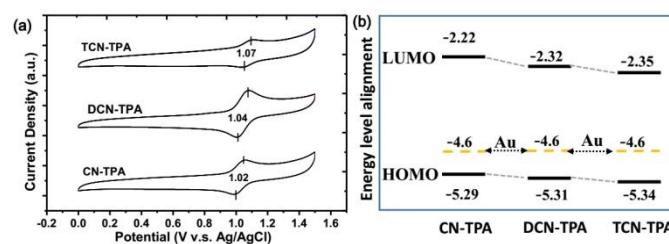


Figure 3 Cyclic voltammograms of CN-TPA, DCN-TPA and TCN-TPA (a), and their energy levels compared with Au Fermi level (b).

Cyclic voltammetry measurement is further carried out to investigate the electron richness of the core and the effect of the added substituents. As shown in Figure 3a, the oxidation potential is 1.02 eV, 1.04 eV, and 1.07 eV for CN-TPA, DCN-TPA and TCN-TPA based on the redox potential (see the marked line). The increasing number of phenyl nitrile substitutes on the TPA core likely impair the electron abundance at the core, resulting in the oxidation reaction occurred at a higher bias. By comparing with ferrocene ($E_{(1/2)}\text{Fc}/\text{Fc}^+ = 0.53$ eV), the HOMO energy levels for CN-TPA, DCN-TPA and TCN-TPA are estimated to be -5.29 eV, -5.31 eV, and -5.34 eV ($\text{HOMO} = -(E_{\text{ox}} + 4.8 - E_{(1/2)}\text{Fc}/\text{Fc}^+) \text{ eV}$)^[12]. The band gaps for three molecules can also be deduced from their absorption edges^[9] (see Figure 2a), which are 3.07 eV, 2.99 eV, and 2.99 eV. Correspondingly, their LUMOs can be obtained by comparing their HOMOs with band gaps. The DFT calculated HOMO/LUMO energies are also listed for comparison (Figure S5). The energy level diagram for three molecules with respect to the Au Fermi level is shown in Figure 3b, clearly HOMO is the preferred conducting orbital to mediate the hole transport^[26]. This is consistent with our assumption previously based on the property of the substituent and the conductance trend measured for DCN-TPA and TCN-TPA. It is worth noting that the conductance in phenyl rings terminated with cyanide linkers normally occur primarily through the LUMO^[27]. In our case of these A-D-A structures, the energy level doesn't change significantly with the added phenyl nitrile groups (ϵ_0 equals 0.71 eV and 0.74 eV for DCN-TPA and TCN-TPA, very close to the I-V results), and their HOMOs maintained a better alignment with the metal Fermi energy than LUMOs. In contrast, the electronic couplings between metal and molecule can be greatly impacted by each addition of the phenyl nitrile group as indicated from the modeling, accounting for the large variation in the measured single-molecule conductance.

In summary, we have designed and synthesized a series of specific A-D-A functional molecules to investigate their single-molecule charge transport properties. The electron-withdrawing feature of the A-type linkers on an electron-rich D-type core could significantly tune the single-molecule conductance by adding extra A-type linkers. Fitting I-V curves with a tunneling model reveals a slightly changed energy barrier for DCN-TPA and TCN-TPA, but a large change (~3 times) in metal-molecule electronic coupling is obtained, which primarily accounts for the conductance difference of up to an order of magnitude between DCN-TPA and TCN-TPA. Photo-physical characterizations, electrochemical measurements of all three molecules are conducted to understand the intramolecular charge transfer properties of these similar-structured molecules which are supportive to the conductance results. This work demonstrates the feasibility and applicability to investigate the electrical properties of emitting molecules via SMCM, paving a new avenue to testify the device performance of functional materials and guide the fabrication process from a single-molecule perspective.

We acknowledge financial support from the National Natural Science Foundation of China (NNSFC) (21705122), Key Project of Hubei Provincial Department of Education (D20191102).

Conflicts of interest

There are no conflicts to declare.

Notes and references

- (a) X. Li, Ming Liu, Y. Li, X. Cai, D. Chen, K. Liu, Y. Cao and S.-J. Su, *Chem. Commun.*, 2016, **52**, 14454; (b) X. Zhan, Z. Wu, Y. Lin, Y. Xie, Q. Peng, Q. Li, D. Ma and Z. Li, *Chem. Sci.*, 2016, **7**, 4355-4363
- (a) X. Liang, Z.-L. Tu, Y.-X. Zheng, *Chem-Eur J*, 2020, **25**, 5623; (b) Y. Chen, J.-J. Zhu, Y. Wu, J. Yao, D. Yang, X. Qiao, Y. Dai, Q.-X. Tong, D. Ma, *J. Mater. Chem. C*, 2020, **8**, 7543; (c) Y. Li, Z. Wang, X. Cai, K. Liu, J. Dong, S. Chang, S.-J. Su, *Dyes and Pigments*, 2019, **163**, 249; (d) S. Izumi, H. F. Higginbotham, A. Nyga, P. Stachelek, N. Tohnai, P. Silva, P. Data, Y. Takeda, and S. Minakata, *J. Am. Chem. Soc.*, 2020, **142**, 1482.
- (a) B. Xu and N. J. Tao, *Science*, 2003, **301**, 12214; (b) Y. Li, M. Buerkle, G. Li, A. Rostamian, H. Wang, Z. Wang, D. R. Bowler, T. Miyazaki, L. Xiang, Y. Asai, G. Zhou & N. Tao, *Nat. Mater.*, 2019, **18**, 357
- (a) L. Chen, Y.-H. Wang, B. He, H. Nie, R. Hu, F. Huang, A. Qin, X. Zhou, Z. Zhao, and B. Z. Tang, *Angew. Chem. Int. Ed.*, 2015, **54**, 4231; (b) N. T. Kim, H. Li, L. Venkataraman, and J. L. Leighton, *J. Am. Chem. Soc.*, 2016, **138**, 11505.
- (a) S. T. Schneebeli, M. Kamenetska, Z. Cheng, R. Skouta, R. A. Friesner, L. Venkataraman, and R. Breslow, *J. Am. Chem. Soc.*, 2011, **133**, 2136; (b) B. Xiao, F. Liang, S. Liu, J. Im, Y. Li, J. Liu, B. Zhang, J. Zhou, J. He and S. Chang, *Nanotechnology*, 2018, **29**, 365501
- (a) Z. Xie, I. Baldea, G. Haugstad, and C. D. Frisbie, *J. Am. Chem. Soc.*, 2019, **141**, 497; (b) J. R. Quinn, J. F. Frank. W., L. Venkataraman, M. S. Hybertsen, and R. Breslow, *J. Am. Chem. Soc.*, 2007, **129**, 6714. DOI: 10.1039/D0CC05602B
- (a) M. Banerjee, R. Shukla, and R. Rathore, *J. Am. Chem. Soc.*, 2009, **131**, 1780; (b) A. Borges, J. Xia, S. Liu, L. Venkataraman, and G. C. Solomon, *Nano Lett.*, 2017, **17**, 4436; (c) S. T. Schneebeli, M. Kamenetska, Z. Cheng, R. Skouta, R. A. Friesner, L. Venkataraman, and R. Breslow, *J. Am. Chem. Soc.*, 2011, **133**, 2136.
- (a) J.-C. Mao, L.-L. Peng, W.-Q. Li, F. Chen, H.-G. Wang, Y. Shao, X.-S. Zhou, X. Zhao, H.-J. Xie, and Z. Niu, *J. Phys. Chem. C*, 2017, **121**, 1472; (b) J. Liu, X. Zhao, Q. Al-Galiby, X. Huang, J. Zheng, R. Li, C. Huang, Y. Yang, J. Shi, D. Z. Manrique, C. Lambert, M. R. Bryce, W. Hong, *Angew. Chem. Int. Ed.*, 2017, **56**, 13061.
- J. Dong, Z. Gong, Y. Li, F. Meng, R. Chen, S. Chang, S.-J. Su, *Opt. Mater.*, 2020, **99**, 109573.
- Q. Zhang, J. Li, K. Shizu, S. Huang, S. Hirata, H. Miyazaki, and C. Adachi, *J. Am. Chem. Soc.*, 2012, **134**, 1470613
- Y. Li, X.-L. Li, D. Chen, X. Cai, G. Xie, Z. He, Y.-C. Wu, A. Lien, Y. Cao, and S.-J. Su, *Adv. Funct. Mater.*, 2016, **38**, 6904.
- Y. Li, Z. Wang, X. Li, G. Xie, D. Chen, Y.-F. Wang, C.-C. Lo, A. Lien, J. Peng, Y. Cao, and S.-J. Su, *Chem. Mater.*, 2015, **27**, 1100.
- G. Xie, X. Li, D. Chen, Z. Wang, X. Cai, D. Chen, Y. Li, K. Liu, Y. Cao, and S.-J. Su, *Adv. Mater.*, 2016, **28**, 181.
- W. Hong, D. Z. Manrique, P. Moreno-García, M. Gulcur, A. Mishchenko, C. J. Lambert, M. R. Bryce, and T. Wandlowski, *J. Am. Chem. Soc.*, 2012, **134**, 2292
- A. Borges, E.-D. Fung, F. Ng, L. Venkataraman, and G. C. Solomon, *J. Phys. Chem. Lett.*, 2016, **7**, 4825.
- (a) L. Yu, Z. Wang, H. Chen, J. Guo, M. Zhang, Y. Liu, J. He, and S. Chang, *ACS Appl. Nano Mater.*, 2020, **3**, 3410; (b) H. Chen, Y. Li, and S. Chang, *Anal. Chem.*, 2020, **9**, 6423.
- Y. Li, B. Xiao, R. Chen, H. Chen, J. Dong, Y. Liu and S. Chang, *Chem. Commun.*, 2019, **55**, 8325.
- L. Venkataraman, Y. S. Park, A. C. Whalley, C. Nuckolls, M. S. Hybertsen, and M. L. Steigerwald, *Nano Lett.*, 2007, **7**, 502.
- S. Guo, J. Hihath, I. Díez-Perez, and N. Tao, *J. Am. Chem. Soc.*, 2011, **133**, 1918.
- (a) Y. Kim, T. Pietsch, A. Erbe, W. Belzig, and E. Scheer, *Nano Lett.*, 2011, **11**, 3734; (b) J. C. Cuevas, & E. Scheer, *Molecular Electronics: An Introduction to Theory and Experiment*
- T. Yelin, R. Korytár, N. Sukenik, R. Vardimon, B. Kumar, C. Nuckolls, F. Evers and O. Tal, *Nat. Mater.*, 2016, **4**, 440.
- Y. Komoto, S. Fujii, H. Nakamura, T. Tada, T. Nishino, M. Kiguchi, *Sci. Rep.*, 2016, **6**, 26606.
- M. Frei, S. V. Aradhya, M. S. Hybertsen, and L. Venkataraman, *J. Am. Chem. Soc.*, 2012, **134**, 9, 4003.
- Z. Xie, I. Baldea, and C. D. Frisbie, *J. Am. Chem. Soc.*, 2019, **141**, 18182.
- J. Ye, Z. Chen, M.-K. Fung, C. Zheng, X. Ou, X. Zhang, Y. Yuan, and C.-S. Lee, *Chem. Mater.*, 2013, **25**, 2630.
- (a) P. Reddy, S.-Y. Jang, R. A. Segalman, & A. Majumdar, *Science*, 2007, **315**, 1568; (b) J. R. Widawsky, P. Darancet, J. B. Neaton, & L. Venkataraman, *Nano Lett.*, 2012, **12**, 354.
- J. Koga, Y. Tsuji, and K. Yoshizawa, *J. Phys. Chem. C*, 2012, **116**, 20607.